The Phase Formation at Mechanically Alloyed Ti-Al Compounds

St. Lauer, Z. Guan, H. Wolf, and Th. Wichert

Technische Physik, Universität des Saarlandes, D-66041 Saarbrücken, Germany

Abstract

The local electric field gradients were used for the investigation of ordered atomic structures in Ti-Al compounds using the radioactive probe ^{111}In. The observed electric field gradients were identified by the comparison with the electric field gradients of the intermetallic compounds γ-TiAl and τ-TiAl$_3$, prepared by conventional melting techniques, or by comparison with X-ray diffraction data. Mechanical alloying of elemental Ti and Al powders was used for the production of Ti$_{0.50}$Al$_{0.50}$ and Ti$_{0.25}$Al$_{0.75}$ powders. Annealing these samples at 1060 K led to the formation of γ-TiAl and τ-TiAl$_3$, respectively. Additionally, the phase Ti$_2$AlN was detected in both cases indicating the incorporation of N impurity atoms. A metastable face centred tetragonal structure was observed in a Ti$_{0.50}$Al$_{0.50}$ sample milled for 4 h and tempered at 880 K. In the case of the Ti$_{0.25}$Al$_{0.75}$, a metastable compound with a lattice structure of the D0$_{23}$ type was formed in the temperature range between 690 K and 1020 K.

Introduction

Ti-Al compounds are promising materials for high temperature applications because of their high melting point, low density, and good oxidation resistance. The widespread use of Ti-aluminides, however, is hindered, up to now, by the lack of ductility and fracture toughness at low temperatures and by the lack of creep resistance at high temperatures [1].

In order to improve the mechanical properties, the process of mechanical alloying has been thoroughly investigated [2]. The advantages of this method are: Powders are the final product enabling the application of powder metallurgical preparation methods, such as net shaping. From the small particle size improved mechanical properties are expected. E.g. metastable amorphous phases [3] or supersaturated solid solutions [4,5] can be produced in contrast to ingot metallurgy. Using a reactive gas or liquid during the milling process, the precipitation of additional phases, such as Ti$_2$AlN [6,7] or Ti$_4$Al$_2$C$_2$ [8], can be achieved.

In this paper, mechanically alloyed Ti-Al compounds were investigated using perturbed γγ angular correlation spectroscopy (PAC) and X-ray diffraction (XRD). With reference to a radioactive probe atom, e.g. ^{111}In, PAC spectroscopy yields information about the short range order, XRD about the long range order. The formation of metastable phases and intermetallic compounds at higher temperatures as well as the incorporation of N-impurities was of special interest in this study.

Experimental details

In a PAC experiment, the electric field gradient (efg) is measured at the site of the probe atom yielding information about its local environment; that means about the formation of new phases, the probe atom is part of, or about the presence of contaminations, if they are present in the neighbourhood of the probe atom. In its principle axis system, the traceless efg tensor V_{ii} is completely described by two quantities: the largest component V_{zz} and the asymmetry parameter $\eta = (V_{xx}-V_{yy})/V_{zz}$. If $|V_{xx}| \leq |V_{yy}| \leq |V_{zz}|$ is chosen, the relation $0 \leq \eta \leq 1$ holds. The used probe atom ^{111}In decays to an excited nuclear state of its daughter isotope ^{111}Cd (Fig. 1). Through the emission of γ_1, the I = 5/2 nuclear level is populated, which has a lifetime of $\tau = 123$ ns. The

emission probability of the second quantum γ_2 with respect to γ_1 is spatially anisotropic due to the conservation of angular momentum during the decay process. The efg is observable via its hyperfine interaction with the nuclear quadrupole moment Q of the $I = 5/2$ level, because it effects a modulation of the emission probability of γ_2 detected at a fixed angle θ with respect to γ_1. The modulation is governed by three frequencies ω_1, ω_2, and $\omega_3 = \omega_1 + \omega_2$, which are proportional to the product QV_{zz} (Fig. 1). The strength of the efg is usually expressed by the quadrupole coupling constant $\nu_Q = eQV_{zz}/h$. The coupling constant ν_Q is determined from ω_1, the asymmetry parameter η from the ratio ω_2/ω_1. In a PAC experiment, the number of coincidences as a function of the time t passed between the emission of the two γ quanta is recorded. Eliminating the exponential function, which describes the decay of the $I = 5/2$ nuclear level, the spectrum is described by:

$$R(t) = A_2 \cdot \left\{ f \cdot \left(s_0 + \sum_{n=1}^{3} s_n \cos \omega_n t \right) + (1 - f) \right\}$$

From the R(t) time spectrum the three frequencies ω_1, ω_2, and ω_3 are extracted yielding the efg parameters. The amplitude of the modulation described by the parameter f reflects the fraction of probe atoms residing in an environment that produces a particular non-zero efg. The fraction of probe atoms exposed to a zero efg is denoted by (1-f). A more detailed description of PAC spectroscopy is found elsewhere [9].

Fig. 1: Decay scheme of the PAC probe ^{111}In.

For the XRD experiments the K_α radiation of Mo or Cu of a Siemens D5000 θ-θ diffractometer was used. The XRD investigations were performed at samples that were treated identically to the samples investigated by PAC, except for the fact that no radioactive ^{111}In was added. The grain size of nanocrystalline samples was determined from the broadening of the diffraction peaks according to the method of Williamson and Hall [10].

Mechanical alloying was performed by milling elemental powders of Ti (purity 99.98 %) and Al (99.99 %) in a Spex 8000 ball mill. The elemental powders were mixed in the compositions 50 at% Ti - 50 at% Al and 25 at% Ti - 75 at% Al and filled into sealed hardened steel vials. The handling of the powders and the milling were performed in a glove-box under Ar atmosphere.

The radioactive ^{111}In probe atoms were incorporated into the Ti-Al samples by diffusion in a sealed quartz tube under a vacuum of 10^{-5} mbar. The diffusion was performed at $T_{diff} = 690$ K for 16 h. Subsequently, the samples were annealed for 16 h at temperatures up to $T_a = 1160$ K. After each step, a PAC spectrum was recorded at 295 K.

Additionally, powders of the intermetallic compounds γ-TiAl and τ-Ti$_3$Al were investigated by PAC as reference samples. The γ-TiAl was produced by the PIGA technique [11] at the GKSS research institute in Geesthacht and τ-TiAl$_3$ was purchased from Goodfellow.

Results and discussion

1.) Reference samples

Samples of the intermetallic compounds γ-TiAl and τ-TiAl$_3$ were diffused with ^{111}In and investigated by PAC. The PAC time spectra R(t) and the corresponding Fourier transforms F(ω) are shown in Fig. 2. In the case of γ-TiAl, the frequency triplet corresponds to an efg that is characterised by $\nu_Q = 142$ MHz and $\eta = 0$ (Fig. 2a), which is known to be caused by the tetragonal L1$_0$ structure of γ-TiAl [12]. It is assumed that ^{111}In
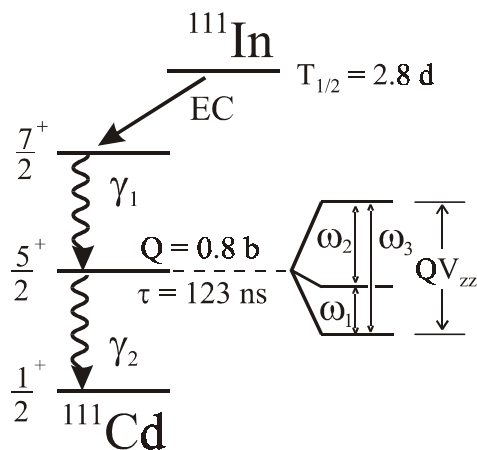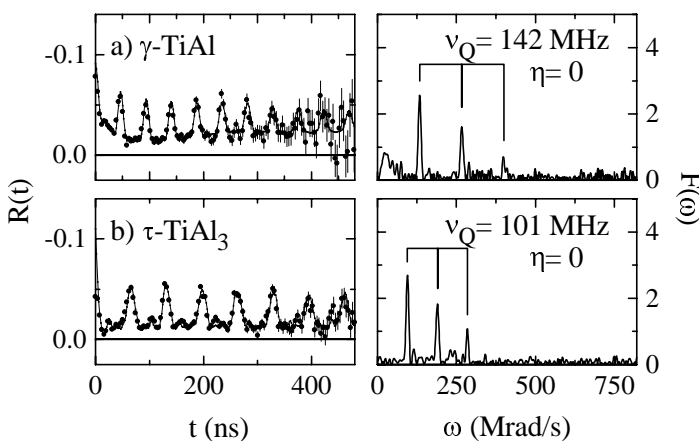

Fig. 2: PAC spectra of the intermetallic compounds γ-TiAl and τ-TiAl$_3$.

2

a) γ-TiAl (tetragonal L1$_0$ structure)
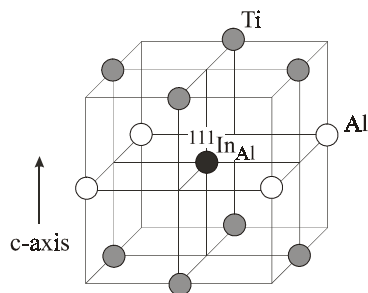
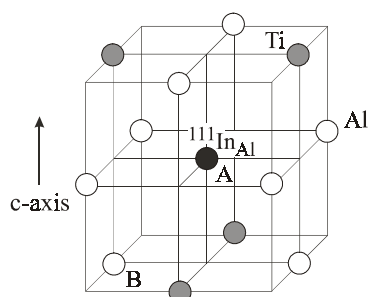b) τ-TiAl$_3$ (tetragonal D0$_{22}$ structure)

Fig. 3: Lattice structures of γ-TiAl and τ-TiAl$_3$. In case of τ-TiAl$_3$ only a half of the unit cell is shown.

is incorporated on the site of the isovalent Al (Fig. 3a).

The PAC spectrum of ^{111}In in τ-TiAl$_3$ shows also a single efg, which is characterised by $\nu_Q = 101$ MHz and $\eta = 0$ (Fig. 2b). The tetragonal D0$_{22}$ structure of τ-TiAl$_3$ contains two non-equivalent Al sites (A and B in Fig. 3b). Both of them can be occupied by ^{111}In resulting in two different axially symmetric efg (i.e. $\eta = 0$). The occurrence of only one efg, however, clearly shows that only one site is occupied by ^{111}In. Taking into account the different atomic radii of Al, Ti, and In, it is suggested that ^{111}In is located at site A, because of the larger distances to the neighbouring Ti atoms as compared to site B. The differing distances are caused by the tetragonal distortion of the τ-TiAl$_3$ lattice. On the other hand, the assumption that ^{111}In is incorporated on the Ti site can not be excluded completely, because it would explain the observation of only one efg and the large ^{111}In atom would be surrounded by twelve smaller Al atoms. However, the observed efg can be used as a fingerprint, in order to detect the formation of τ-TiAl$_3$.

2.) Mechanically alloyed Ti$_{0.50}$Al$_{0.50}$

Elemental powder blends of the composition 50 at% Ti - 50 at% Al were mechanically alloyed by ball milling for 4 h (sample A) and 13 h (sample B). After a milling time of 4 h, an XRD analysis still shows the presence of elemental Ti and Al via their characteristic diffraction peaks. These peaks disappear in case of sample B milled for 13 h and a supersaturated solid solution with an hcp structure is observed in accordance with [4,5]. The development of this hcp solid solution is explained by Klassen and co-workers in terms of the dissolution of Al into the hcp Ti lattice [13]. The width of the diffraction peaks indicates a nanocrystalline microstructure with a grain size of about 20 nm.

After diffusion of ^{111}In into the solid solution of sample B, the subsequent PAC measurement shows a distribution of efg (Fig. 4a), which indicates the incorporation of ^{111}In atoms at non-equivalent sites. On one hand, this observation may suggest that ^{111}In probes are located in the grain boundaries of the material. On the other hand, if the ^{111}In atoms are located in the crystalline grains, the absence of chemical order leading to different atomic configurations of Ti and Al atoms around the ^{111}In atoms and resulting in different efg would explain the observed frequency- or efg-distribution. Annealing sample B at 880 K, the occurrence of two efg (Fig. 4b) indicates the formation of two different ordered structures. The fraction of ^{111}In atoms in these structures increases at higher annealing temperatures and becomes maximal at $T_a = 1060$ K. At the same time, the efg distribution has completely disappeared (Fig. 4c). The first efg corresponds to γ-TiAl (Fig. 2a), the second efg, which is characterised by $\nu_Q = 259$ MHz and $\eta = 0$, was not observed before. The corresponding XRD pattern of sample B (Fig. 5) exhibits tetragonal γ-TiAl and, additionally, the
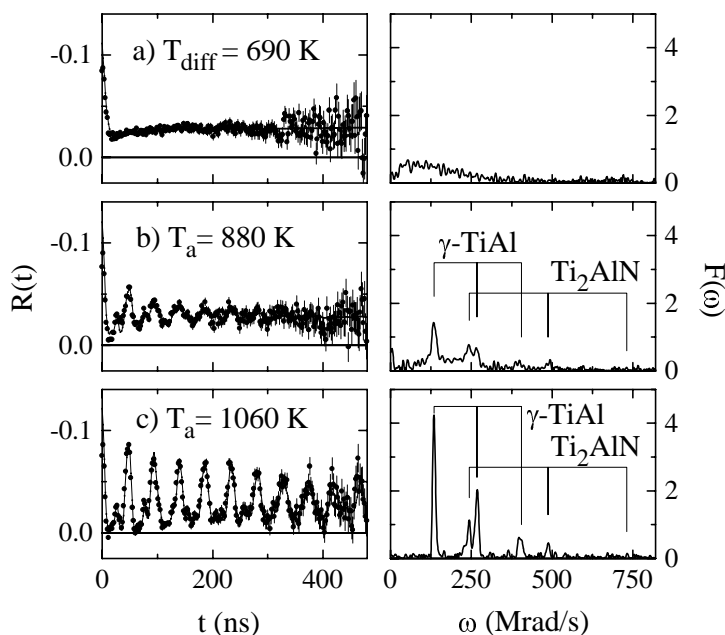

Fig. 4: PAC spectra of Ti$_{0.50}$Al$_{0.50}$ milled for 13 h. The spectra were recorded after diffusion at 690 K and annealing at 880 K and 1060 K.
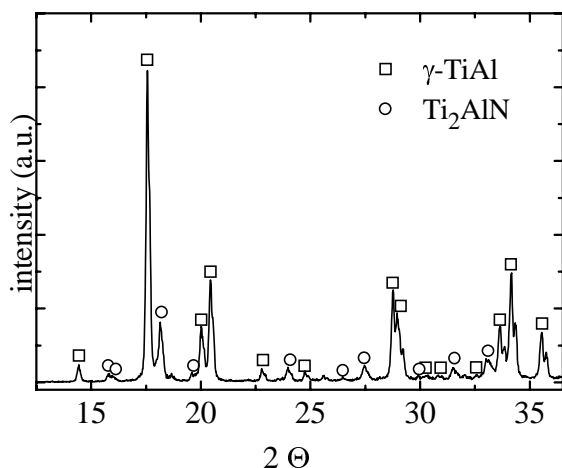
Fig. 5: XRD pattern of $Ti_{0.50}Al_{0.50}$ milled for 13 h and annealed at 1060 K. (K_α radiation: Mo)

phase Ti_2AlN with a hexagonal structure of τ-$AlCCr_2$ type. Comparing the results obtained by PAC and XRD, the new efg characterised by $\nu_Q = 259$ MHz is attributed to the phase Ti_2AlN. Detailed investigations in dependence of the milling time show an increasing amount of Ti_2AlN with increasing milling time [14]. Thus it is concluded that the residual contamination of the Ar atmosphere in the glove-box gives rise to the N atoms, which are incorporated into the Ti-Al alloy during ball milling. The N-contamination of the primary Ti and Al powders would not explain the increasing impurity level with increasing milling time. The formation of the ordered compound Ti_2AlN occurs during the tempering of the sample and enables the detection by PAC. Other impurities such as O, H, or Fe, which are possibly dissolved in the Ti-Al host lattice, are not detected by PAC.

Following diffusion of ^{111}In at 690 K into the $Ti_{0.50}Al_{0.50}$ sample milled for 4 h (sample A), the PAC spectrum shows an efg distribution as in the case of sample B. Annealing at 880 K leads to the formation of a new local structure as indicated by the new efg, characterised by $\nu_Q = 57$ MHz and $\eta = 0.1$ (Fig. 6a). The equilibrium phase γ-TiAl is observed by PAC, when sample A was tempered at 1060 K (Fig. 6b). At the same time, no Ti_2AlN is detected, indicating a weaker contamination with N as observed in sample B. Obviously the milling time strongly affects the amount of N in the samples.

Directly after the milling process, XRD shows that the powder consisted of both hcp and fcc crystallites as indicated by the diffraction peaks of Ti and Al. After

Fig. 6: PAC spectra of $Ti_{0.50}Al_{0.50}$ milled for 4 h. The spectra were recorded after annealing at 880 K and 1060 K.

annealing at 1060 K, the equilibrium phase γ-TiAl is formed. The structure observed at 880 K therefore is attributed to a metastable intermediate structure, which is formed during the interdiffusion of Ti and Al. The new efg observed by PAC clearly indicates that the local structure is different from γ-TiAl. The lattice structure was analysed by XRD (Fig. 7). Besides minor unidentified structures, the diffraction pattern shows a face centred lattice structure with a slight tetragonal distortion (fct). The XRD-data, however, cannot give information about the degree of chemical order.
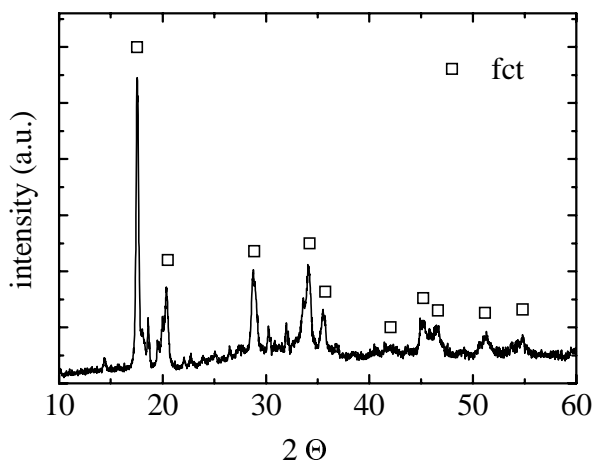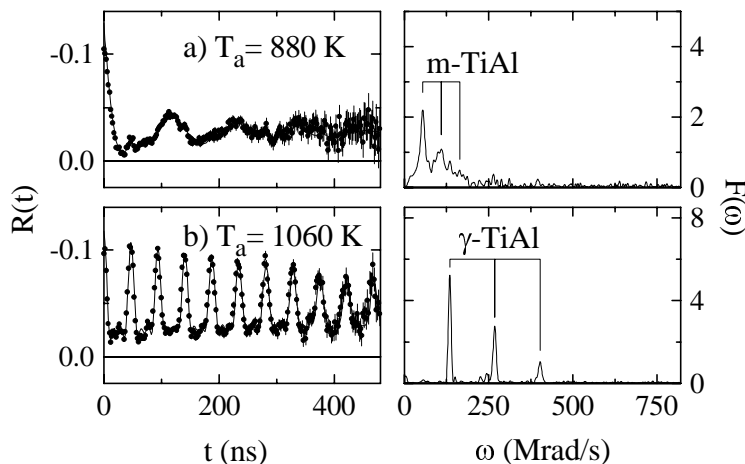
3.) Mechanically alloyed $Ti_{0.25}Al_{0.75}$

Mechanical alloying of a powder blend at the composition 25 at% Ti - 75 at% Al after a milling time of 31 h (sample C) resulted in a nanocrystalline solid solution with a fcc lattice (Fig. 8a) in accordance with the observations of Oehring et al. [4]. The grain size was determined to be about 20 nm from the width of the diffraction
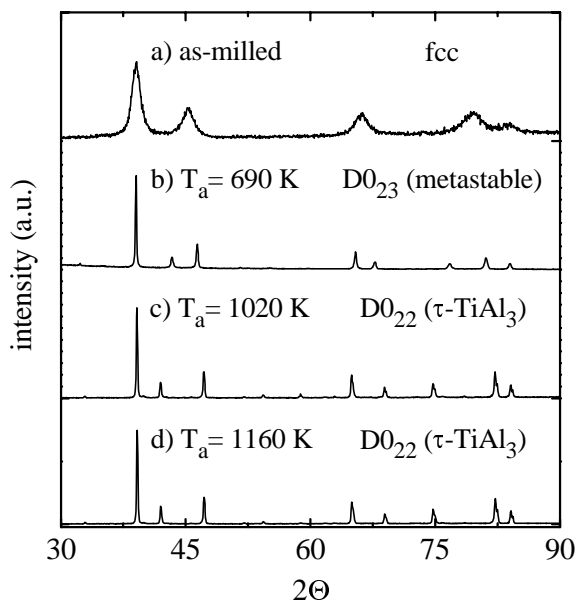

Fig. 7: XRD pattern of $Ti_{0.50}Al_{0.50}$ milled for 4 h and annealed at 880 K. (K_α radiation: Mo)

Fig. 8: XRD patterns of $Ti_{0.25}Al_{0.75}$ milled for 31 h. The patterns were recorded after the milling process and after annealing at 690 K, 1020 K, and 1160 K. (K_α radiation: Cu)

peaks. Following tempering of the mechanically alloyed powder at 690 K, the XRD pattern indicates the formation of a metastable ordered $TiAl_3$ phase with a tetragonal $D0_{23}$ structure (Fig. 8b). The occurrence of a metastable $D0_{23}$ phase in the temperature range of about 700 K was already observed on Ti-Al multilayers of the composition 25 % Ti - 75 % Al [15]. Increasing the temperature to 1020 K, the equilibrium phase τ-$TiAl_3$, having a $D0_{22}$ structure, is formed (Fig. 8c).

The PAC experiments performed at sample C show different results, which are not in agreement with the XRD data. Following diffusion of ^{111}In into the $Ti_{0.25}Al_{0.75}$ sample, no well-defined efg, indicating an ordered structure, is observed by PAC, whereas the XRD analysis showed the formation of the ordered metastable $D0_{23}$ structure. Subsequent tempering at 880 K shows 5 % of the ^{111}In atoms to be incorporated on equivalent sites giving rise to two different efg, denoted by I and II in Fig. 9a (see Table 1). Up to now, it is not clear, which structures these two efg can be assigned to. Aft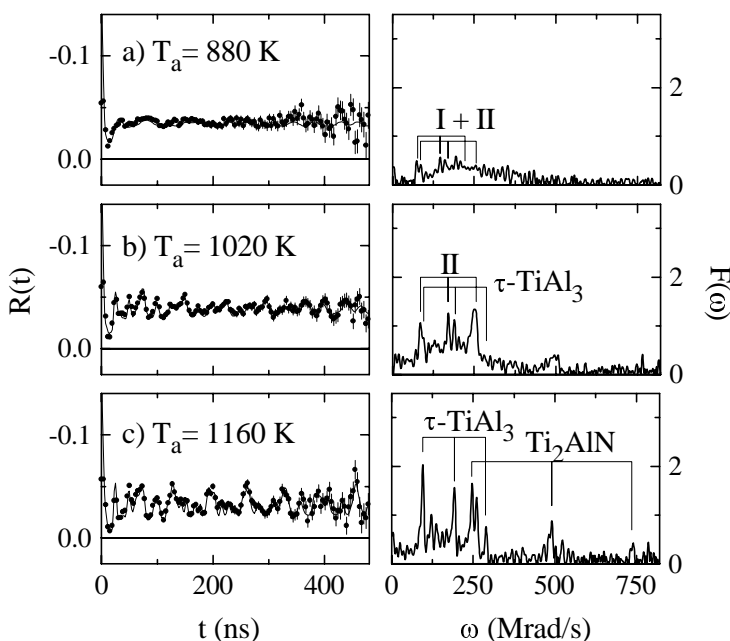er increasing the temperature to 1020 K, which should lead to the formation of the equilibrium phase τ-$TiAl_3$, the PAC spectrum shows only a fraction of 5 % of ^{111}In atoms to be located in τ-$TiAl_3$ (Fig. 9b). The fraction of probe atoms, incorporated in the τ-$TiAl_3$ lattice, increases to 15 %, when the sample is tempered at 1160 K and, additionally, the signal of Ti_2AlN appears (Fig. 9c) indicating the presence of N-impurities via the formation of the Ti_2AlN phase. This phase, however, was not detected by XRD.

The complementary investigations of $TiAl_3$ compounds by applying PAC and XRD clearly show the different sensitivities of both experimental techniques. A metastable $D0_{23}$ phase and subsequently the equilibrium phase τ-$TiAl_3$ are identified by XRD, whereas the PAC investigation shows ordered structures only to a small extent. On the other hand, the formation of Ti_2AlN is observed by PAC, but not by XRD. The fact that the ordered crystalline structures are not observed by PAC may be explained by the preferential incorporation of the ^{111}In probes in the grain boundaries, which results in an efg distribution. On the other hand, the formed Ti_2AlN grains may be too small to be identified by XRD, but large enough for the observation by PAC because of its short range sensitivity.

Summary

The sensitivity of perturbed $\gamma\gamma$ angular correlation spectroscopy to locally ordered atomic structures containing ^{111}In probe atoms was applied to the investigation of mechanically alloyed $Ti_{0.50}Al_{0.50}$ and $Ti_{0.25}Al_{0.75}$ compounds. As reference, the efg of γ-TiAl and τ-$TiAl_3$ were measured at the respective intermetallic compound prepared by conventional melting techniques. In case of $Ti_{0.50}Al_{0.50}$, complete alloying, that

Fig. 9: PAC spectra of $Ti_{0.25}Al_{0.75}$ milled for 31 h. The spectra were recorded after annealing at 880 K, 1020 K, and 1160 K.

means the formation of an hcp solid solution, was achieved following ball milling for 13 h (sample B). Annealing this sample at 1060 K led to the formation of γ-TiAl and, additionally, of Ti_2AlN, which revealed the incorporation of N atoms during ball milling. After a milling time of only 4 h (sample A), XRD still showed the lattice structures of Ti and Al. Annealing this sample at 880 K resulted in the formation of a metastable structure (m-TiAl) with fct lattice structure.

Table 1 : Electric field gradients observed in the different Ti-Al compounds.

designation	ν_Q	η	structure	sample
γ-TiAl	142 MHz	0	intermetallic γ-TiAl	reference sample, $Ti_{0.50}Al_{0.50}$
τ-TiAl$_3$	101 MHz	0	intermetallic τ-TiAl$_3$	reference sample, $Ti_{0.25}Al_{0.75}$
Ti_2AlN	259 MHz	0	Ti_2AlN	$Ti_{0.50}Al_{0.50}$, $Ti_{0.25}Al_{0.75}$
m-TiAl	57 MHz	0.1	metastable structure	$Ti_{0.50}Al_{0.50}$ (sample A)
I	77 MHz	0	?	$Ti_{0.25}Al_{0.75}$
II	90 MHz	0	?	$Ti_{0.25}Al_{0.75}$

In case of the $Ti_{0.25}Al_{0.75}$ sample milled for 31 h, a metastable $D0_{23}$ phase and the equilibrium phase τ-TiAl$_3$ with a $D0_{22}$ structure were observed by XRD after annealing between 690 K and 1020 K. The PAC results showed that only up to 40 % of the ^{111}In atoms were incorporated into locally ordered structures. The formation of Ti_2AlN following annealing was detected by PAC but could not be observed by XRD.

Acknowledgements

References

1.) P. Nash, H. Kim, H. Choo, H. Ardy, S.J. Hwang, and A.S. Nash, Material Science Forum **88-90** (1992), p. 97
2.) T. Itsukaichi, K. Masuyama, M. Umemoto, I. Okane, and J.G. Cabañas-Moreno, J. Mater. Res. **8** (1993), p. 1817
3.) S. Kobayashi and H. Kimura, Material Science Forum **88-90** (1992), p. 97
4.) M. Oehring, T. Klassen, and R. Bormann, J. Mater. Res. **8** (1993), p. 2819
5.) G. Walkowiak, T. Sell, and H. Mehrer, Z. Metallkd. **85** (1994), p. 332
6.) K.Y. Wang, J.G. Wang, and G.L. Chen, J. Mater. Res. **10** (1995), p. 1247
7.) Y. Chen, A. Calka, J.S. Williams, and B.W. Ninham, Materials Science and Engineering **A187** (1994), p. 51
8.) T. Suzuki, T. Ino, and M. Nagumo, Material Science Forum **88-90** (1992), p. 639
9.) Th. Wichert and E. Recknagel, in "Microscopic Methods in Metals", ed. U. Gonser, Topics in Current Physics **40** (1986), p. 317
10.) G.K. Williamson and W.H. Hall, Acta Metall. **1** (1953), p. 22
11.) GKSS, annual report, Geesthacht 1993
12.) J. Fan and G.S. Collins, Hyp. Int. **79** (1993), p. 745
13.) T. Klassen, M. Oehring, and R. Bormann, J. Mater. Res. **9** (1994), p. 47
14.) St. Lauer, Z. Guan, H. Wolf, and Th. Wichert, submitted to Journal of Materials Research
15.) C. Michaelsen, S. Wöhlert, R. Bormann, and K. Barmak, Mat. Res. Soc. Symp. Proc. **398** (1996), p. 245